

# Beam dynamics simulations of the transverse-to-longitudinal emittance exchange proof-of-principle experiment at the Argonne Wakefield Accelerator

M. Rihaoui\*, W. Gai<sup>†</sup>, K-J-Kim<sup>†</sup>, P. Piot\*\*, J. G. Power<sup>†</sup> and Y.-E Sun<sup>‡</sup>

*\*Department of Physics and Northern Illinois Center for Accelerator & Detector Development,  
Northern Illinois University, IL 60115 DeKalb, USA*

*<sup>†</sup>HEP Division, Argonne National Laboratory, Argonne, IL 60439, USA*

*\*\*Department of Physics and Northern Illinois Center for Accelerator & Detector Development,  
Northern Illinois University, IL 60115 DeKalb, USA*

*and Accelerator Physics Center, Fermi National Accelerator Laboratory, Batavia IL 60510, USA*

*<sup>‡</sup>Accelerator Physics Center, Fermi National Accelerator Laboratory, Batavia IL 60510, USA*

**Abstract.** Transverse-to-longitudinal emittance exchange has promising applications in various advanced acceleration and light source concepts. A proof-of-principle experiment to demonstrate this phase space manipulation method is currently being planned at the Argonne Wakefield Accelerator. The experiment focuses on exchanging a low longitudinal emittance with a high transverse horizontal emittance and also incorporates room for possible parametric studies e.g. using an incoming flat beam with tunable horizontal emittance. In this paper, we present realistic start-to-end beam dynamics simulation of the scheme, explore the limitations of this phase space exchange.

**Keywords:** photoinjector, phase space manipulation, beam dynamics

**PACS:** 29.27.-a, 41.85.-p, 41.75.F

## INTRODUCTION & THEORETICAL BACKGROUND

State-of-art photoemission sources based on rf-gun – photoinjectors – are capable of producing electron beams with low 6-D emittance. Typically the longitudinal and transverse emittance have very different value and it might be advantageous for specific applications to exchange one of the transverse emittance with the longitudinal emittance. A method to perform such manipulation was first suggested in Reference [1], and proposed in Reference [2] as a scheme to suppress microbunching instability in high brightness electron linacs. The method was later refined and adapted to improve the performance of single-pass free-electron lasers (FELs) [3, 4]. The transverse-to-longitudinal emittance exchange is an intricate manipulation which requires a thorough proof-of-principle experiment before confidently incorporating it in the design of next generation accelerators. Such an experiment is planned at the Argonne wakefield accelerator (AWA) [5] and at the Fermilab A0 facility [6].

The emittance exchanger under consideration in this paper is composed of a horizontally-deflecting cavity flanked by two doglegs [4]. The exchange occurs between the horizontal and longitudinal phase spaces. We therefore work in the four-dimensional space and consider an electron with coordinate  $\mathbf{X}^i = (x, x', z, \delta)$  where  $x, x'$

are the conjugated horizontal trace space coordinates,  $z$  the longitudinal coordinate and  $\delta$  the fractional momentum spread. We take a horizontally bending dogleg that consists of two rectangular dipoles, with respective bending angles  $\pm\theta$ , separated by a drift of length  $D$ . The transfer matrix corresponding to one dogleg is

$$M_{DL}(\eta, R_{56}, L) = M_B(L_b, -\theta)M_D(D)M_B(L_b, \theta) = \begin{bmatrix} 1 & L & 0 & \eta \\ 0 & 1 & 0 & 0 \\ 0 & \eta & 1 & R_{56} \\ 0 & 0 & 0 & 1 \end{bmatrix}, \quad (1)$$

where  $M_B$  and  $M_D$  respectively correspond to the transfer matrices of a bending dipole with length  $L_b$  and bending angle  $\theta$  and of a drift of length  $D$ . The total path length is  $L \equiv [D + 2L_b c(\theta)]/[c^2(\theta)]$ , the dispersion  $\eta \equiv 1/[c^2(\theta)s(\theta)] \times [2L_b c(\theta)(1 - c(\theta)) + Ds^2(\theta)]$  and the longitudinal dispersion  $R_{56} \equiv 1/[c^2(\theta)s(\theta)] \times [-2\theta L_b c^2(\theta) + L_b s(\theta)c(\theta) + Ds^3(\theta)]$ . We use the shorthanded notation  $\{c, s\}(\theta) \equiv \{\cos, \sin\}(\theta)$ .

The horizontally-deflecting cavity operates on the  $\text{TM}_{110, \pi}$  mode and consists of  $1/2 + 1 + 1/2$  cells. The associated transfer matrix, adapted from Reference [11], is

$$M_{cavity}(\kappa, L_c, \lambda) = \begin{bmatrix} 1 & L_c & \frac{\kappa L_c}{2} & 0 \\ 0 & 1 & \kappa & 0 \\ 0 & 0 & 1 & 0 \\ \kappa & \frac{\kappa L_c}{2} & \frac{23}{128}(\kappa^2 \lambda) & 1 \end{bmatrix}, \quad (2)$$

where  $\kappa$  is the deflecting cavity strength and  $L_c$  is the total length of the cavity including two drifts of length similar to the pipes used in the electromagnetic model [12]. When the condition  $\kappa = -1/\eta$  is satisfied, the total transfer matrix of the exchanger takes the form

$$M_{EX}^T = \begin{bmatrix} 0 & \frac{23\lambda}{128} & -\xi & \eta - R_{56}\xi \\ 0 & 0 & -\frac{1}{\eta} & -\frac{R_{56}}{\eta} \\ -\frac{R_{56}}{\eta} & \eta - R_{56}\xi & \frac{23R_{56}\lambda}{128\eta^2} & \frac{23R_{56}^2\lambda}{128\eta^2} \\ -\frac{1}{\eta} & -\xi & \frac{23\lambda}{128\eta^2} & \frac{\lambda R_{56}}{128\eta^2} \end{bmatrix} \equiv \begin{bmatrix} A & B \\ C & D \end{bmatrix}, \quad (3)$$

where  $\xi \equiv \frac{128L + 64L_c - 23\lambda}{128\eta}$ . The final transverse and longitudinal emittances are given by

$$\begin{bmatrix} \epsilon_x^2 \\ \epsilon_z^2 \end{bmatrix} = \begin{bmatrix} |A|^2 & |B|^2 \\ |C|^2 & |D|^2 \end{bmatrix} \begin{bmatrix} \epsilon_{x,0}^2 \\ \epsilon_{z,0}^2 \end{bmatrix} + \lambda^2 \epsilon_{x,0} \epsilon_{z,0} I, \quad (4)$$

where  $I$  is the  $2 \times 2$  identity matrix and  $\lambda^2$  is a coupling term. Under the thin lens approximation a perfect emittance exchange is achieved [i.e.  $|A| = |D| = 0$  and  $|B| = |C| = 1$ ]. In general, i.e. including thick lens effects, the coupling term can be minimized by a proper choice of either initial longitudinal or transverse Courant-Snyder (C-S) parameters. Here we opt for minimizing  $\lambda$  with respect to the initial longitudinal C-S parameters. Since the bunch length (i.e.  $\beta_{z,0}$ ) is fixed by the gun settings,  $\lambda$  is minimized with respect to the correlated fractional momentum spread, i.e..  $\alpha_{z,0} = -\langle z_0 \delta_0 \rangle / \epsilon_{z,0}$ .

The optimum value,  $\alpha_{z,0,m} = \beta_{z,0}/R_{56}$ , corresponds to a longitudinal phase space chirp  $d\delta_0/dz_0 = -1/R_{56}$  that produces a minimum bunch length at the cavity location. Such a choice results in a negligible value for the coupling term  $\lambda^2$ .

## VALIDATION OF FIRST ORDER TRANSFER MATRIX

The proof-of-principle experiment currently under design will be conducted at the AWA. The accelerator includes a 1+1/2 cell 1.3 GHz rf gun followed by a 22-cell standing wave 1.3 GHz linac operating on the  $TM_{010,\pi/2}$  mode. The emittance exchanger will be installed  $\sim 1.5$  m downstream of the linac; see Fig. 1. Four quadrupoles located between the linac and the exchanger can be used to tune the C-S parameters at the entrance of the emittance exchanger. The beam dynamics in the emittance exchanger is modeled with IMPACT-T which incorporates a 3-D quasi-static space charge algorithm [8]. The deflecting cavity is simulated with HFSS [?] and the so-generated 3-D electromagnetic field maps were imported in IMPACT-T. The vertical magnetic field of the horizontally-bending rectangular dipoles for the doglegs were provided by the manufacturer [9]. These fields were used to accurately model the dipoles in IMPACT-T by fitting the fringe field regions with eight-order Enge functions.

A first step in the numerical modeling is to check how the inclusion of realistic fields in the model alter the first order single-particle model described in the previous section (where all the fields are idealized and assumed to follow hard edge models). To find the first order transfer matrix of the system modeled in IMPACT-T we use a

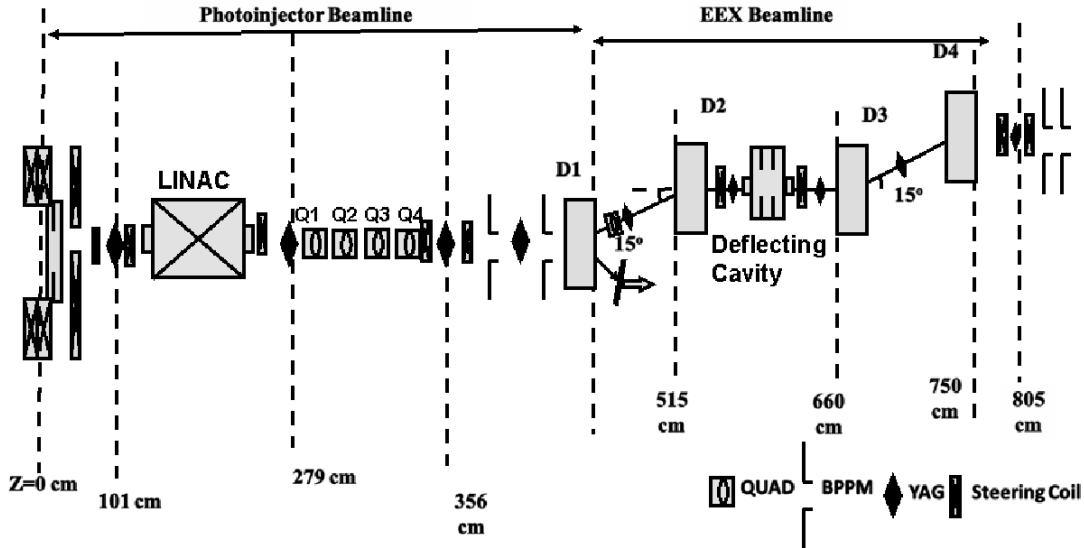


FIGURE 1. Overview of the AWA photoinjector with the emittance exchanger beamline.

set of six macroparticles each displaced along one coordinate by a small amount  $\delta\mathbf{X}^i$  with respect to a reference particle. This initial displacement is mapped, downstream of the exchanger, as a displacement  $\delta\mathbf{X}^{i,j} = M_i^j \delta\mathbf{X}^i$ , where  $M_i^j$  is the first order transfer matrix associate to the exchanger; thereby providing the needed information to extract

the transfer matrix elements. Using this technique we inferred the transfer matrix of the emittance exchanger in the  $(x, x', z', \delta)$  phase space to be

$$M_{EX}^S = \begin{bmatrix} -0.0010 & 0.0858 & 8.4 & -0.266 \\ -0.0015 & 0.015 & 3.896 & 0.2355 \\ 0.2387 & 0.2471 & 0.0233 & 0.0022 \\ 3.896 & 8.409 & 0.745 & 0.0436 \end{bmatrix}. \quad (5)$$

The matrix numerically computed from Equation 3 is

$$M_{EX}^T = \begin{bmatrix} 0 & 0.041 & 8.3 & -0.2456 \\ 0 & 0 & 3.909 & 0.236 \\ 0.236 & 0.2456 & 0.038 & 0.002 \\ 3.909 & 8.3 & 0.631 & 0.0382 \end{bmatrix}. \quad (6)$$

We therefore observe a decent agreement between the ideal analytical transfer matrix and the transfer matrix inferred from the IMPACT-T model. The matrix devised from the numerical model also satisfies the symplectic condition.

## BEAM DYNAMICS CALCULATIONS

A key point of the proposed experiment is to exchange a small longitudinal emittance with a larger horizontal emittance. We therefore need to find a proper tuning of the AWA injector to provide such an emittance partition. The simulation of the injector were done with ASTRA using the  $(r, z)$  cylindrical symmetric space charge algorithm [10]. ASTRA was used in conjunction with a genetic optimizer to seek possible settings for the injector that would provide emittance partitions  $\varepsilon_x/\varepsilon_z > 3$  with the constraints on emittances  $5 < \varepsilon_x < 20 \mu\text{m}$  and  $\varepsilon_z < 5 \mu\text{m}$  [7]. Several possible tunes were found and an example of achieved parameters is shown Fig. 2. The formalism described in the first Section is

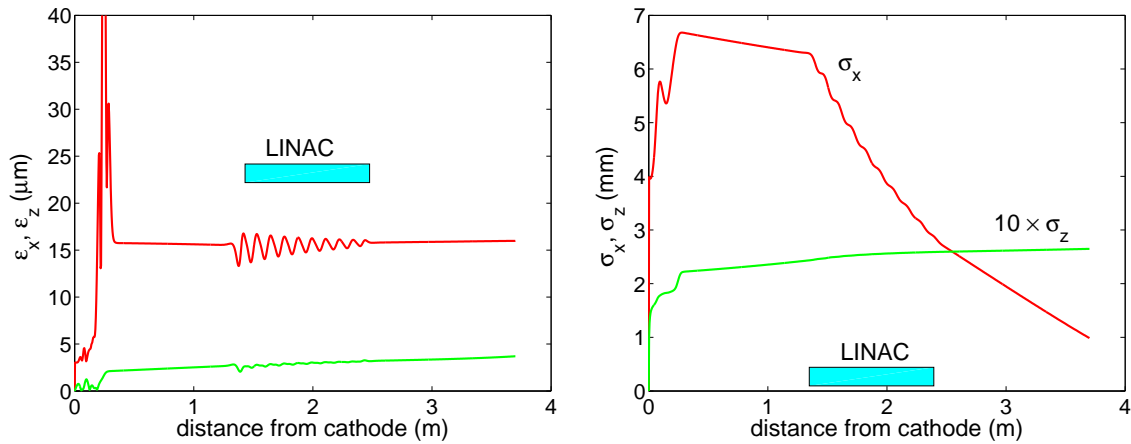


**FIGURE 2.** Emittances (left) and beam sizes (right) evolutions along the AWA injector beamline up to  $z = 3.70$  m. The achieve emittance partition is  $(\varepsilon_x, \varepsilon_y, \varepsilon_z) = (15.4, 15.4, 3.4) \mu\text{m}$ .

based on linear transfer matrix. We explore higher order effects with the aid of numerical

simulations. A 6-D Gaussian beam distribution with given transverse C-S parameters  $(\alpha_{x,y}, \beta_{x,y})$  and emittances  $\varepsilon_{x,y}$ , and longitudinal phase space parametrized by the bunch length  $\sigma_z$ , chirp  $d\delta/dz$  and emittance  $\varepsilon_z$  is generated via a Sobol sequence and tracked with IMPACT-T without including space charge effects.

The longitudinal phase space parameters are in principle fixed (the bunch length is given and the chirp need to be tuned to  $-1/R_{56}$ ; see first Section), only the transverse C-S parameters can be varied given an incoming emittance partition. An example of transverse and longitudinal relative emittance dilutions respectively defined as  $\delta_x \equiv \varepsilon_x/\varepsilon_{x0} - 1$  and  $\delta_z \equiv \varepsilon_z/\varepsilon_{z0} - 1$  are shown in Fig. 3 as a function of incoming transverse horizontal C-S parameters. These plots point to an optimum range of horizontal C-

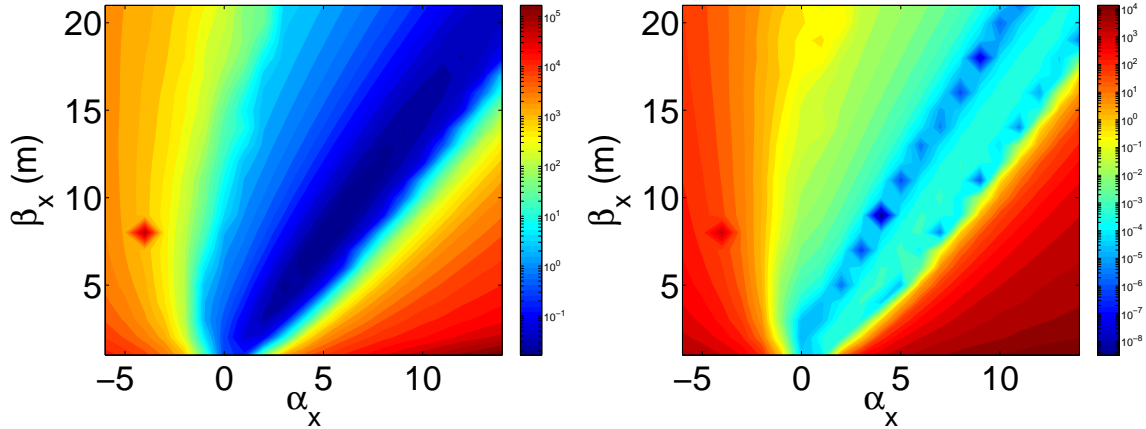


**FIGURE 3.** Transverse (left) and longitudinal (right) relative emittance dilution at the exit of the exchanger beamline versus the incoming horizontal Courant-Snyder beam parameters respectively referred to as  $\delta_x$  and  $\delta_z$ ; see text for details.

S parameters needed to be achieved upstream of the exchanger an almost complete transverse-to-longitudinal emittance exchange. The smaller emittance dilution arises from second order effects mainly via nonlinear coupling between the transverse and longitudinal degrees of freedom, i.e  $T_{ij6}$ ,  $T_{ij5}$ . This was checked with ELEGANT [13] simulations by comparing results obtained from first and second order tracking studies. Given the incoming C-S parameters at the booster cavity exit, the four quadrupoles are tuned to match the horizontal C-S parameters to the required values. There is no particular requirement on the vertical C-S parameters: they should be chosen to avoid particle loss in the exchanger beamline.

An example of realistic single-particle dynamics simulation of the exchanger corresponding to the distribution shown in Fig. 2 is presented in Fig. 4. In these calculations we observe a significant emittance dilution in  $x$ . The apparent disagreement with Fig. 3, which predicts the final transverse emittance to match the incoming longitudinal emittance within  $\sim 10\%$  when proper C-S parameters are used, is due to emittance dilution in the quadrupoles and can be improved with a refined matching algorithm which takes into account this emittance dilution. The emittance dilution in the quadrupoles comes from chromatic aberrations (given the incoming energy spread, the  $\beta$  functions in the quadrupoles are too high). Nevertheless, even in the worst case scenario shown in Fig. 4, a clear signature of the exchange should be observed. When space charge force

are included the emittance dilution in the horizontal plane increases by another 50%, this growth should be alleviated by a proper choice of C-S parameters.

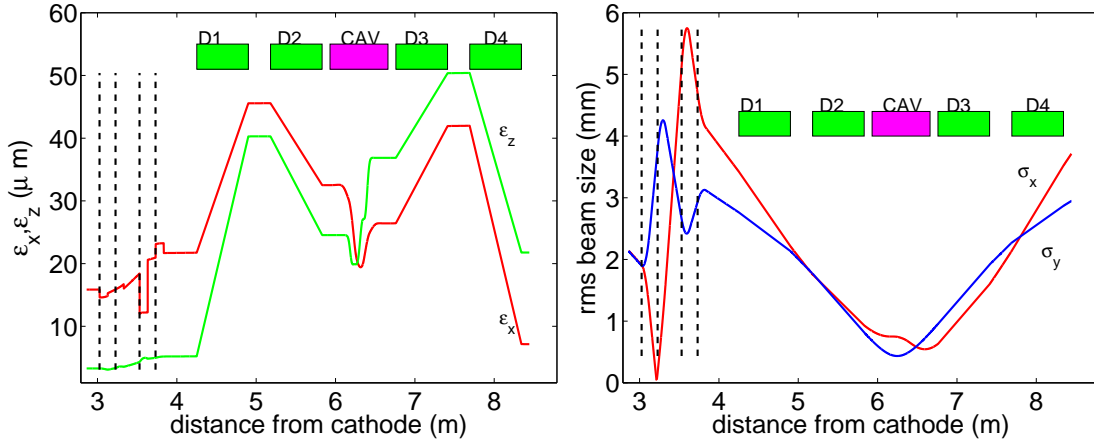


**FIGURE 4.** Emittances (left) and beam sizes (right) evolutions along the exchanger beamline. The achieve emittance partition at the exchanger entrance is  $(\epsilon_{x0}, \epsilon_{y0}, \epsilon_{z0}) = (21.73, 17.88, 5.21) \mu\text{m}$ . The final emittance partition is  $(\epsilon_x, \epsilon_y, \epsilon_z) = (7.16, 18.06, 21.77) \mu\text{m}$ . The dashed vertical lines indicated the locations of the quadrupoles (Q1,Q2,Q3,Q4) in Figure 1. The green (D1,D2,D3,D4) and magenta rectangles respectively indicate the locations of the four dipoles and the deflecting cavity.

## ACKNOWLEDGMENTS

The work of M. R. and P. P. was supported by the US Department of Energy under Contract No. DE-FG02-04ER41323 with Northern Illinois University. The work of W. G., K.-J. K and J. G. P was supported Argonne National Laboratory under Contract No. DE-AC02-06CH11357 with the U.S. Department of Energy. The work of Y.-E S. was supported by the Fermi Research Alliance, LLC under Contract No. DE-AC02-07CH11359 with the U.S. Department of Energy.

## REFERENCES

1. Y. Orlov et al., Proc. of PAC91, San Francisco, 2838 (1991).
2. M. Cornachia, and P. Emma, *Phys. Rev. ST Accel. Beams* **6** 030702 (2003).
3. K.-J. Kim and A. Sessler, AIP Conf. Proc. **821**, p. 115 (2006).
4. P. Emma, Z. Huang, K.-J. Kim, and P. Piot, *Phys. Rev. ST Accel. Beams* **9**, 100702 (2006).
5. Y.-E Sun, et al, Proc. of the PAC07, 3441 (2007).
6. R. Fliller, et al. , Proc. 13th Advanced Accelerator Concepts Workshop, Santa Cruz, CA (2008).
7. H. Shang, [http://www.aps.anl.gov/Accelerator\\_Systems\\_Division/Operations\\_Analysis/index.shtml](http://www.aps.anl.gov/Accelerator_Systems_Division/Operations_Analysis/index.shtml)
8. J. Qiang, S. Lidia, R. D. Ryne and C. Limborg-Deprey, *Phys. Rev. ST Accel. Beams* **9**, 044204 (2006).
9. G. Andonian (RadiaBeam), private communication (2007).
10. K. Flöttmann, ASTRA user manual, available at the www address <http://www.desy.de/~mpyflo/>
11. D. A. Edwards, "Notes on transit in deflection mode pillbox cavity" (unpublished) (2007).
12. J. Shi et al., Proc. of EPAC08, Genoa, (Italy), 916 (2008).
13. M. Borland, "elegant: A Flexible SDDS-Compliant Code for Accelerator Simulation," Advanced Photon Source LS-287 (2000).